

Inflatable Cylinders for Deployable Space Structures

M. Schenk¹, S.G. Kerr², A.M. Smyth², S.D. Guest²

¹Surrey Space Centre, University of Surrey, Guildford, United Kingdom, M.Schenk@surrey.ac.uk

²Department of Engineering, University of Cambridge, United Kingdom (Corresponding Author: sdg@eng.cam.ac.uk)

Summary: Inflatable space structures offer the prospect of compact stowed large light-weight structures, which can be inflated to their full dimensions once in space. After inflation the structures may be rigidised to ensure long term structural performance without the need to maintain the internal pressure. Inflatable cylindrical booms are an important category of space inflatable, and often form the structural members of larger structures. A promising method of compactly packaging inflatable cylindrical booms is the use of origami fold patterns. The geometry of the selected fold pattern affects the deployment characteristics of the boom. By modeling the fold pattern as a mechanism of hinged plates, a simple geometric incompatibility can be taken as a measure of the material strains during deployment; this approach enables the initial selection of suitable fold patterns. A series of experiments is set up to investigate the efficacy of the strain-rigidisation of the aluminium-laminate material used for the inflatable cylinders, and study the deployment characteristics of different cylindrical fold patterns. The work in this paper forms part of the InflateSail project to design a large inflatable satellite de-orbiting device to be launched on a 3U CubeSat.

Keywords: inflatable space structures, cylindrical booms, origami, kinematics

INTRODUCTION

As space debris accumulates in low earth orbit (LEO), the likelihood of collisions increases. With each collision generating further debris, this may lead to a cascade of further collisions, thus jeopardizing future space missions. In order to avoid this scenario, debris growth mitigation and removal of space debris have become active areas of research. One approach to debris reduction is to reduce the de-orbiting time of defunct satellites by the use of large, light-weight structures (often referred to as gossamer structures) to increase the aerodynamic drag of the satellite. This ensures that the satellite de-orbits and disintegrates in the atmosphere, rather than forming a potential source of future space debris.

The work described in this paper forms part of the 'InflateSail' project¹, which aims to develop a large inflatable sail structure for use as a satellite de-orbiting device. A flight demonstration mission is planned for the 'QB50' launch scheduled for 2015, using a 3U CubeSat. The limited satellite dimensions (100x100x340mm) impose severe demands on the packaging efficiency of the deployable structure. In order to deploy a large gossamer structure from the confines of a CubeSat, the InflateSail project will therefore make use of inflatable structural components. Space inflatables have been in development since the 1960s and offer the enticing prospect of compact stowage of large deployable space structures.

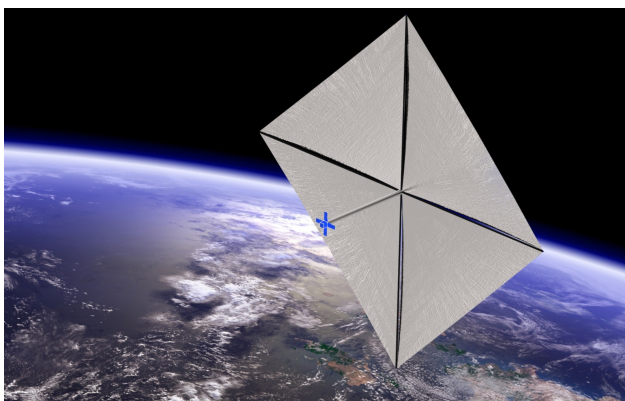


Figure 1: impression of a proposed InflateSail design with a single inflatable boom providing an offset between the CubeSat and the sail structure; the sail membrane is supported by four tape-spring booms. Image credit: Gordon McKenzie.

The overall structural concept of InflateSail is under development, but a key component will be the use of inflatable cylindrical booms as structural members; see **Figure 1**. The booms will have a thin cylindrical

skin which is folded for launch, with the boom then inflated for deployment. The skin is rigidised following deployment to ensure that long-term maintenance of the internal pressure is unnecessary; the rigidisation is achieved by overinflating the cylinder to cause controlled yielding to a metal-polymer laminate skin. The inflation gas is provided by Cool Gas Generators (CGGs), in which the gas is stored in a solid form, giving the benefit of reliable long term storage [13]. The selected CGG is expected to generate 5g of N₂ (equivalent to 3.4 litres at STP), which will be released over a period of approximately 10 seconds to inflate the structure. The relatively rapid release of inflation gas is an important design driver, and has led to the selection of origami patterns (see **Figure 2**) as a potential packaging method for the inflatable cylindrical booms used for InflateSail.

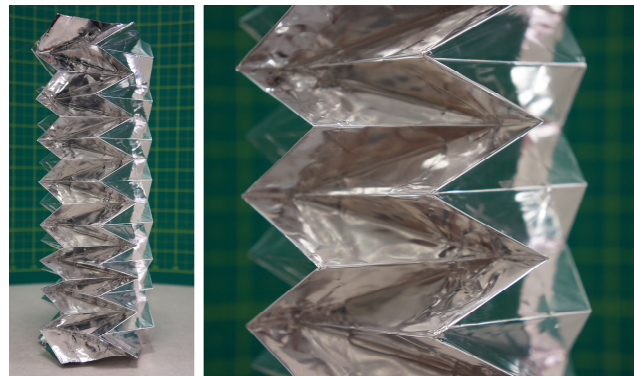


Figure 2: an origami boom in a partly deployed configuration (fully deployed diameter and height: 95 and 500mm).

The paper is laid out as follows. A discussion of inflatable origami cylinders precedes the description of the geometry of a family of fold patterns based on reverse folds, and a simplified analysis the deployment kinematics. Some preliminary experimental results and manufacturing methods are discussed, and directions for future work are indicated.

ORIGAMI FOLDED CYLINDERS

A promising approach to compactly stow an inflatable deployable boom, is the use of *origami patterns*, where the developable cylindrical surface is formed into flat facets joined by fold lines [6, 12, 17, 24]; the facets pop through into the final cylindrical form at the end of inflation. A key consideration for the application of origami patterns in InflateSail is their open cross-section in the stowed configuration, allowing for rapid dispersal of the inflation gas and fast deployment of the boom. Moreover, origami booms have been shown to combine compact stowage with straight-line deployment [11, 15].

¹ <http://www.deploytech.eu/>

Alternative packing methods for inflatable booms include *z-folding*, *coiling* and *conical-telescopic folding*. The classic *z-fold* offers simplicity of packing, but suffers from an unpredictable deployment path due to the discrete compartments formed by the folds [3, 16]. Coiling the booms around a cylindrical hub provides a linear deployment [2, 18], but the tip rotation precludes applications where multiple booms are interconnected. Lastly, by introducing a slight taper to the boom, it can be inverted and everted at regular intervals to form a compact telescopic stowed configuration, with an open cross-section and straight deployment [21]. During deployment the concentric folds must travel along the boom; preliminary investigations showed that the necessary plastic strains damaged the metal-laminate foils used for the inflatable booms. As a result, origami folding patterns were selected as a prime candidate for the inflatable booms for InflateSail.

A wide range of folded cylindrical booms has been proposed in the literature. This study is focused on a specific category of fold patterns, consisting of a series of reverse folds that are arranged to form a closed cylindrical cross-section [1, 9, 17]. Not considered here are fold patterns that are oriented helically along the boom [6, 7, 12], as these produce an axial rotation during deployment. The choice of fold pattern will not only affect the packing efficiency, but also the stored strain energy and the deployment characteristics of the inflatable boom. Experiments by Senda *et al.* [15] suggest that the straightness of boom deployment can be linked to the degree of material deformation; however, the link between fold pattern and deployment characteristics was not fully understood.

In the present paper, a geometric/kinematic deployment study precedes any experimental and detailed numerical analysis of the folded booms, as it assists the selection of suitable fold patterns. An important paradigm in engineering origami is *rigid origami*, where it is assumed that the fold pattern can be modelled as rigid panels connected through frictionless hinges. This simplification turns the analysis of origami folding into a study of kinematics. Deformation during deployment of the folded cylinder is then represented by a geometric incompatibility, for example the length of a single fold line [6, 24] or a fold angle [9]. Later in the project, in order to gain more detailed insight into the deployment mechanics and corresponding material deformations, finite element simulations will be necessary. The inflation of *z*-folded, coiled and conically folded booms was studied using FEA [11, 22]; for origami booms, Senda *et al.* [15] provide a stress analysis of a partly-deployed boom under inflation pressure, and Wu and You [23] studied the axial collapse and energy dissipation of thin-walled origami booms. However, no FEA studies of the deployment of inflatable rigidisable origami booms have been found.

In this section the geometry and kinematics of the fold patterns are described, before a simplified strain measure is introduced to quantify the amount of material deformation during deployment.

Reverse Folds

The base element of the cylindrical fold patterns described in this paper is the *reverse fold* shown in **Figure 3**. It consists of four fold lines meeting at a vertex: two fold lines are collinear, with the other two set at an angle φ . The fold has a single degree of freedom, and its folding motion can be described by the fold angle $\alpha \in [0, \pi]$. The variation of the enclosed angle $\beta_1 \in [\pi - 2\varphi, \pi]$ is then given by:

$$\beta_1 = \pi - 2 \cdot \operatorname{atan} \left(\cos \frac{\alpha}{2} \cdot \tan \varphi \right) \quad [1]$$

Multiple reverse folds can be combined; for example, for a double-reverse fold the angle $\beta_2(\alpha)$ is given as follows:

$$\beta_2 = \pi - 2 \cdot \operatorname{atan} \left(\cos \frac{\alpha}{2} \cdot \tan \varphi_1 \right) + 2 \cdot \operatorname{atan} \left(\cos \frac{\alpha}{2} \cdot \tan \varphi_2 \right) \quad [2]$$

It is important to note that this transfer function is not strictly increasing with respect to the fold angle α . This has important consequences for the selection of suitable fold patterns for inflatable cylinders, as detailed later in this section. Further reverse folds can be combined, but the increased number of fold lines meeting at a vertex results in greater local material deformations, and thus an increased risk of tears and pin-hole punctures. In this study only double-reverse folds are considered; in a tessellated fold pattern, this limits the number of folds meeting at a vertex to six.

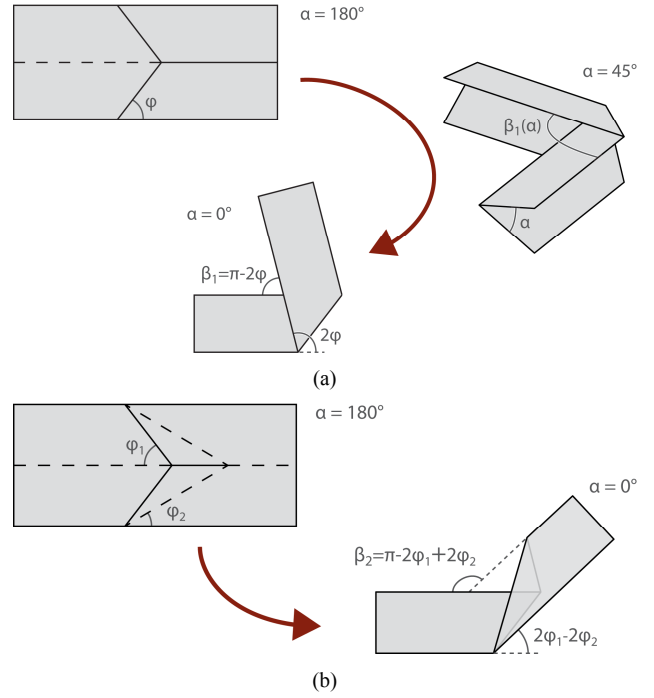


Figure 3: The (a) reverse fold is the basic element of the cylindrical origami patterns. It consists of four fold lines meeting at a vertex: two folds are collinear, with the other two set at an angle φ . As the material is folded from its initial ($\alpha = 180^\circ$) to fully stowed configuration ($\alpha = 0^\circ$) the enclosed angle $\beta_1 \in [\pi - 2\varphi, \pi]$ varies; (b) a double-reverse fold combines two such folds, set at angles $\varphi_1 > \varphi_2$.

Closure Condition

In this study we focus on fold patterns with n repeated *double-reverse folds* forming a closed cross-section. The resulting folded boom will have an n -fold rotational symmetry, and the cylindrical closure condition is thus given by:

$$\beta_2 = \frac{n-2}{n} \cdot \pi \quad [3]$$

While the closure condition can be satisfied for any partly-folded configuration α , we shall here focus on the fully stowed configuration with $\alpha = 0$. This is done to minimize the elastic strain energy in the stowed configuration, which is important for a reliable deployment of the inflatable boom. For the stowed configuration of the double-reverse fold, the closure condition thus provides the following relationship between the angles φ_1 and φ_2 :

$$\varphi_1 - \varphi_2 = \frac{\pi}{n} \quad [4]$$

Henceforth, the angle $\varphi_1 \in [\frac{\pi}{n}, \frac{\pi}{2}]$ is taken as the free design parameter, and φ_2 follows from the number of sides n . During deployment the enclosed angle β_2 of the double-reverse fold will vary according to Equation 2, and the closure condition will no longer be satisfied. In the next section, the incompatibility $\Delta\beta = |\beta - \beta_0|$ will be taken as simple measure for the necessary strain during deployment [9]. After some trigonometric manipulation, Equation 2 and 3 can be rewritten as a quadratic equation in $\cos(\alpha/2)$:

$$\left(\tan^2 \varphi_1 - \tan \varphi_1 \tan \frac{\pi}{n} \right) \cdot \cos^2 \frac{\alpha}{2} - (1 + \tan^2 \varphi_1) \cdot \cos \frac{\alpha}{2} + \tan \varphi_1 \tan \frac{\pi}{n} = 0 \quad [5]$$

Thus, the relationship $\beta_2(\alpha)$ may permit multiple solutions, and a folded boom can be designed to have multiple stable states [6, 9, 24]; see **Figure 5**. This feature opens up the possibility of manufacturing a folded boom in partly-deployed configuration, before compacting it to the fully stowed configuration.

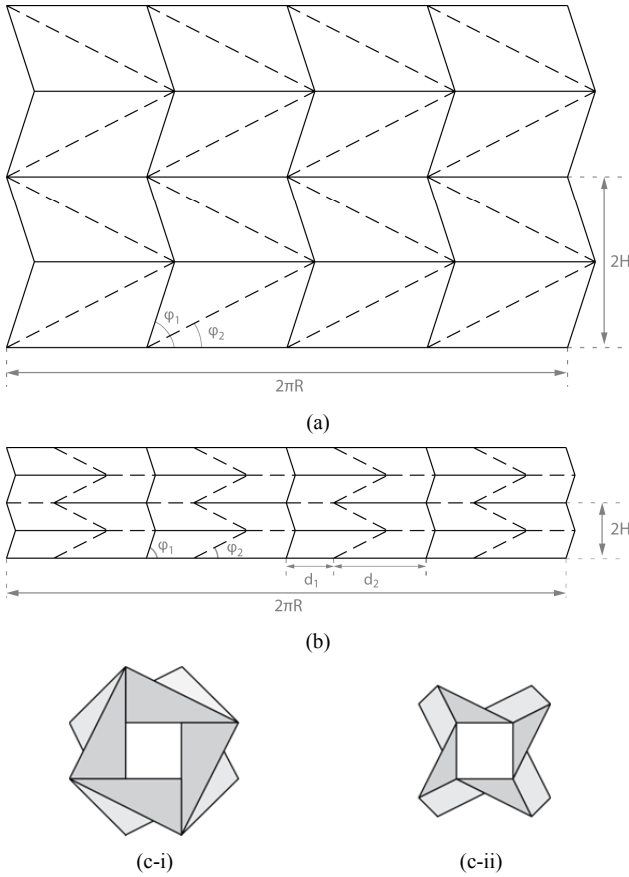


Figure 4: two geometric variations for a fold pattern with $n=4$ and $\varphi_1 = 72^\circ$: the (a) triangulated and (b) a curved Miura pattern. For the latter, the ratio $H/R = 0.31$ is selected according to Equation 9 to minimize the number of overlapping layers in the stowed configuration; (c) cross-section views of the two booms in fully stowed state.

Geometric Variations

A wide range of geometric variations is possible within the family of cylindrical fold patterns based on the n -fold repetition of double-reverse folds [9]. In this study two types are considered; see **Figure 4**.

In the *triangulated* patterns all facets of the fold pattern are (modulo reflection and rotation) identical triangles. For a given n and φ_1 the normalized height H/R of a single repeating layer is given by

$$\frac{H}{R} = \frac{2\pi}{n} \cdot \frac{\tan \varphi_1 \cdot \tan \varphi_2}{\tan \varphi_1 - \tan \varphi_2} \quad [6]$$

and provides an upper bound for other pattern variations. A detailed analysis of the geometry and mechanics of triangulated cylinders is provided in [6-8].

The *curved Miura* pattern introduces spacing between the reverse folds, thereby reducing the number of fold lines at each vertex. For the patterns considered in this study, the relationship between d_1 and d_2 is coupled to ensure identical quadrilateral facets. The fold pattern geometry is then determined by setting the ratio H/R :

$$\frac{d_1}{R} = \frac{\pi}{n} - \frac{1}{2R} \cdot \frac{\tan \varphi_1 - \tan \varphi_2}{\tan \varphi_1 \cdot \tan \varphi_2} \quad [7]$$

with

$$\frac{d_2}{R} = \frac{2\pi}{n} - \frac{d_1}{R} \quad [8]$$

An interesting feature of this fold pattern is the ability to limit the number of overlapping layers per folded ring to four, and thus reduce the packaged height [17]. The required H/R is given by

$$\frac{H}{R} = \frac{2\pi}{n} \cdot \sec \frac{\pi}{n} \cdot \cos \varphi_1 \cdot \sin \left(\varphi_1 - \frac{\pi}{n} \right) \quad [9]$$

and results in

$$\frac{d_1}{d_2} = \frac{\sin(\varphi_1 - \pi/n)}{\sin(\varphi_1 + \pi/n)} \quad [10]$$

As the stowed height is also affected by the number of folds over the boom length (determined by height H of the layers), this provides a trade-off to minimize the overall packaged dimensions.

For the *Miura* patterns, the decreased number of folds per vertex will reduce the local strains at the vertices (and thus may reduce the likelihood of introducing pin-hole punctures), but the increased number of folds results in a greater amount of total stored strain energy. An additional feature of this type of pattern is the radial expansion due to the star-shaped cross-section.

Structural Properties

Using the geometric and kinematic analysis, some insight can be gained into the structural properties of the folded cylindrical boom. Firstly, the deployment strains will be estimated using a simply geometric incompatibility. Secondly, the stored strain energy is estimated based on the total length of fold lines per unit length of the boom.

Deployment Deformations

As described previously, the angle β of the double reverse folds varies during deployment. The geometric incompatibility

$$\Delta\beta = |\beta - \beta_0| \quad [11]$$

can be taken as a simplified measure of the necessary strain during deployment [9, 24]. Consequently, the total deformation per layer is given by $n \cdot \Delta\beta$. By means of illustration, in **Figure 5** is plotted the geometric incompatibility versus the boom deployment ratio,

$$\frac{L}{L_{max}} = \sin \left(\frac{\alpha}{2} \right) \quad [12]$$

for a boom with $n = 4$ for different values of φ_1 .

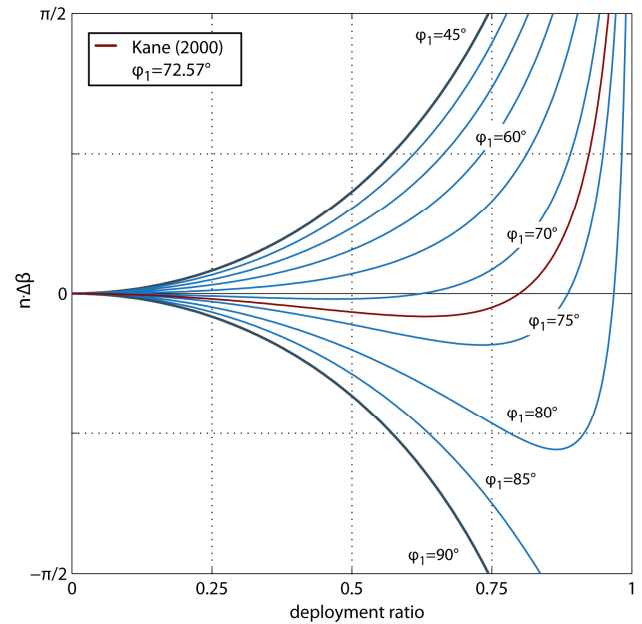


Figure 5: The enclosed angle β of the double reverse-fold will vary with the fold angle α as described by Equation 2. Here is plotted the geometric incompatibility $n \cdot \Delta\beta$ against the deployment ratio, i.e. deployed length/boom length, for booms with $n = 4$. As can be seen, certain fold patterns permit two stable configurations where the geometric incompatibility is zero. A minimum-distortion geometry proposed by Kane [9] is highlighted.

In order to compare the geometric incompatibility during deployment among different geometries, some form of mean deviation may be defined. For example, Kane [9] uses the Root Mean Square (RMS) over a predefined range of the fold angle α . This leaves the question of selecting a suitable integration range: from fully stowed to fully deployed, or to a partly folded configuration? Experimental analysis and

finite element simulations are required to study the deployment behaviour, but minimising the geometric incompatibility over the initial stage of deployment is clearly desirable, more so due to the reduced bending stiffness of the boom at that stage of deployment.

It is here useful to emphasise the benefits of using cylindrical booms with double-reverse folds. For single inversions, the relationship $\beta_1(\alpha)$ is strictly increasing, and the cross-section will therefore deform significantly during deployment. For the double-reverse folds the interplay between the two reverse folds with φ_1 and φ_2 enables a more controlled opening. Nonetheless, the use of fold patterns with a single reverse fold has been explored for inflatable deployable booms [5, 20]. In the case of the TADECS inflatable boom developed by Astrium, a dedicated mechanism ensures a controlled deployment [10].

While the geometric analysis provides a greatly simplified description of the deployment strains, it serves to compare and select potentially suitable fold patterns. For example, Senda *et al.* [15] describe deployment experiments for several fold patterns, including those with single and double inversion folds. The straightness of deployment was linked to the amount of material deformation; this was further supported by the presence of higher stress concentrations in the finite element analysis. In that study the tested *Miura* patterns tested were selected empirically. **Figure 6** shows the fold patterns studied by Senda *et al.* [15], and their geometric incompatibility $n \cdot \Delta\beta$ during deployment. In the experiments from Senda *et al.*, the *Pentalpha* (a) boom showed better straight-line deployment, which is supported by the smaller geometric incompatibility.

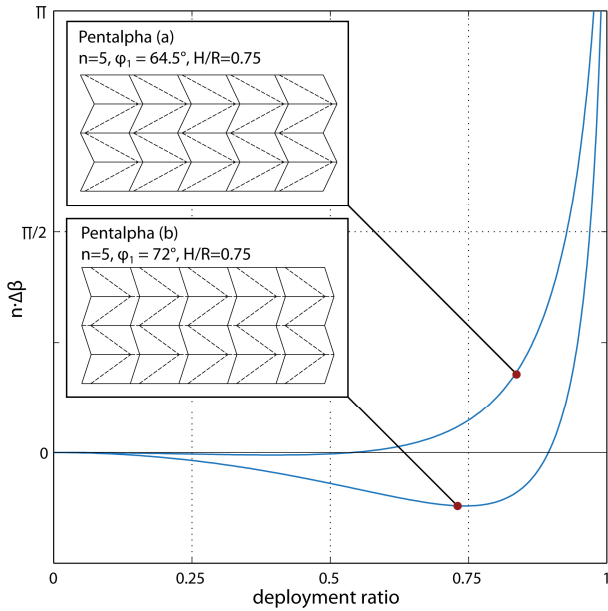


Figure 6: The incompatibility $n \cdot \Delta\beta$ during deployment of two booms studied experimentally by Senda *et al.* [15]. The Pentalpha (a) pattern with $\varphi_1 = 64.5^\circ$ was found to exhibit a better straight-line deployment, which is here supported by the lower geometric incompatibility.

Strain Energy

As a first approximation, the strain energy stored in the stowed configuration is proportional to the length of the fold lines (taking a constant elastic spring back along fold lines). The total length of fold lines is given as:

$$\frac{\Sigma F}{L} = 2\pi \frac{R}{H} + n \cdot \frac{(\sin\varphi_1 + \sin\varphi_2)}{\sin\varphi_1 \cdot \sin\varphi_2} \quad [13]$$

with ΣF the total fold length, L the deployed boom length, and

$$\frac{H}{R} \in \left[0, \frac{2\pi \cdot (\tan\varphi_1 - \tan\varphi_2)}{n \cdot \tan\varphi_1 \cdot \tan\varphi_2} \right] \quad [14]$$

In **Figure 7** is plotted the stored strain energy for a range of fold patterns, over a range of fold angle φ_1 and H/R . Shown are the lowest energy configurations and corresponding number of sides n . For small values of φ_1 a greater number of sides n results in a lower total fold length. For larger values of φ_1 , however, a smaller number of sides n is preferred. It is further important to note that the total fold length – and therefore the approximate strain energy – is independent of the cylinder

radius R . This means that the strain energy density will increase with decreasing boom radius. Further refinement of this analysis should include a term for the strain energy stored in the localised deformations at the vertices.

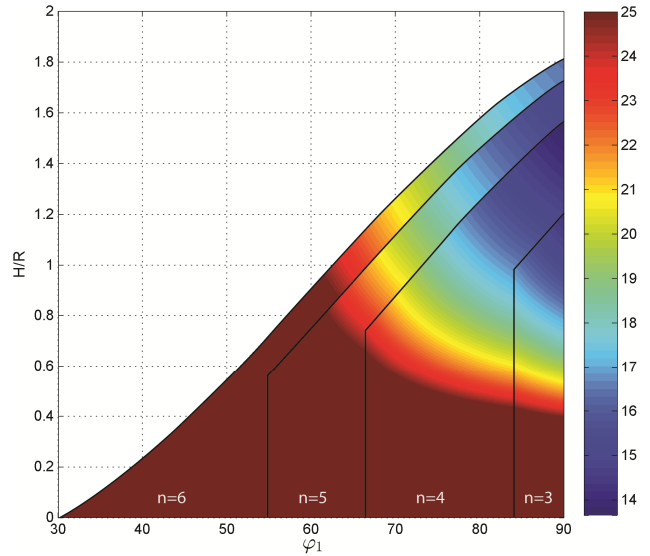
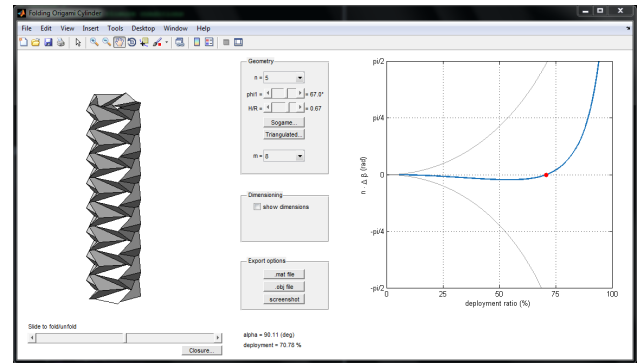


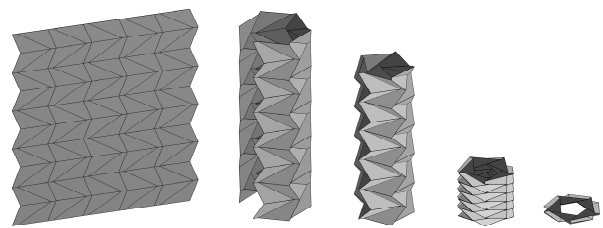
Figure 7: The stored strain energy can be approximated by the total fold length per unit length of boom $\Sigma F/L$ (values >25 have been omitted). For a given combination of φ_1 and H/R the total fold length will depend on the choice of the number of sides n of the fold pattern; the bounded regions indicate the value of n with the lowest strain energy.

Parametric Design Tool

The fold patterns described in this section have been incorporated in a parametric design tool written in Matlab; see **Figure 8**. The software program enables trade-off studies between different fold geometries, and provides the ability to dimension the booms to fit the constraints of a CubeSat. The selected geometry can then be transferred to finite element software for more detailed analysis.



(a)



(b)

Figure 8: A parametric design tool (a) written in Matlab enables rapid exploration of different fold patterns for cylindrical booms; the design parameters φ_1, n and H/R can be varied, and (b) the subsequent fold pattern can be folded/unfolded interactively.

INFLATION EXPERIMENTS

The kinematic analysis in the previous section offers a simplified description of the origami boom deployment. Experiments are necessary to investigate the deployment characteristics of the inflatable origami booms and establish their structural performance after deployment. A key prerequisite is to develop a manufacturing method to accurately fold the origami booms with the desired fold pattern. In this section the strain rigidisation of inflatable booms is outlined, before introducing a manufacturing method for the origami booms, and describing some preliminary results from inflation experiments.

Strain Rigidisation

In the design of inflatable space structures, an important challenge is to ensure long-term structural performance after deployment. In order to avoid problems associated with deflation, the inflatable cylinders will therefore be *rigidised* after inflation. A wide range of rigidisation techniques has been proposed for use in inflatable space structures [14]. The method selected for InflateSail is strain-rigidisation of Aluminium-Mylar laminate foils; see **Figure 9**. After the initial deployment, the laminate is stressed to beyond the yield point of the Aluminium, and the subsequent plastic strains removes the creases associated with the fold pattern. The resultant thin walled cylinder should only have minor defects, and be able to carry load even after deflation; see **Figure 10**.

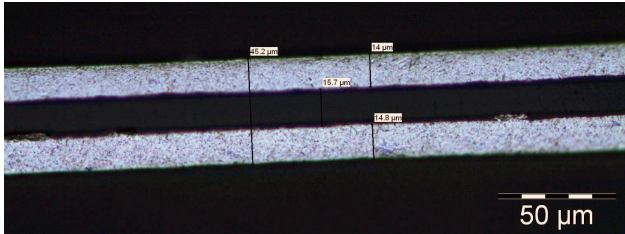


Figure 9: a microscope image of the cross-section of a sample of Aluminium-Mylar laminate foil used for the InflateSail experiments. The laminate foil is made up of approximately 14/14/14μm Al/Mylar/Al separated by thin layers of adhesive.

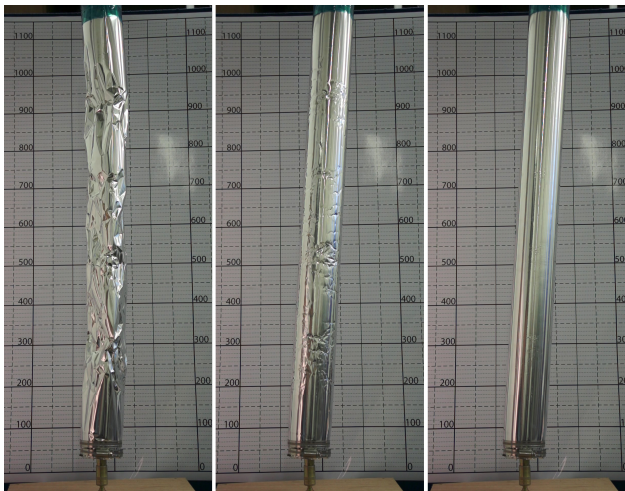


Figure 10: strain-rigidisation an inflatable cylinder: during inflation the creases in the skin material are removed through plastic deformation of the Aluminium layer (boom length 1m; diameter 90mm).

The minimum required rigidisation pressure is straightforwardly estimated. For a closed thin-walled cylinder with radius r , and wall thickness t and inflation pressure P , the longitudinal and hoop skin stress are respectively given by:

$$\sigma_l = \frac{Pr}{2t} \quad [15]$$

and

$$\sigma_h = \frac{Pr}{t} = 2\sigma_l \quad [16]$$

For the onset of plastic deformation in the aluminium layers, a plane stress *Von Mises* yield criterion is assumed

$$\sigma_y = \sqrt{\sigma_1^2 - \sigma_1\sigma_2 + \sigma_2^2} \quad [17]$$

with σ_y the material yield stress, and σ_i the principal stresses. For an inflatable cylinder $\sigma_1 = \sigma_l$, $\sigma_2 = \sigma_h$, resulting in

$$\sigma_y = \sqrt{3} \cdot \sigma_l = \sqrt{\frac{3}{4}} \cdot \frac{Pr}{t} \quad [18]$$

Thus, the pressure required for onset of rigidisation becomes:

$$P_y = \sqrt{\frac{4}{3}} \cdot \frac{\sigma_y t}{r} \quad [19]$$

After depressurization, a residual compressive stress builds up in the aluminium layers, balanced by a tensile stress in the polymer [4]. The extent to which the stiffness and strength of a cylinder can be recovered after packaging must be determined experimentally, and those results will inform the overall structural design for InflateSail. Furthermore, as a fixed quantity of gas will be supplied by the CGGs, the required rigidisation pressure will determine the final boom dimensions.

Manufacture of Origami Booms

The manufacture of origami folded booms is challenging: accurate folding is necessary as the deployment properties are sensitive to the geometric fold parameters; stress concentrations at vertices may lead to pin-hole punctures; reversal of fold direction may result in cracking; during the folding process the boom dimensions and geometry vary, and thus no fixed mandrels can be used. The selected Aluminium-Mylar laminate material introduces a further challenge: the low volume fraction of Mylar results in a small spring back along the fold lines, and the material therefore has no 'memory' of previous fold lines (unlike, say, when folding the cylinders from paper).

One suitable manufacturing process makes use of pre-folded 'master sheets' to accurately fold the cylinder: a sheet of Aluminium-Mylar foil is sandwiched between two pre-folded card sheets, which enforce the folding kinematics. After the fold lines have been transferred to the laminate foil, the sides of the sheets are sealed to form a closed cylinder, which is folded to its fully stowed configuration; see **Figure 11**.

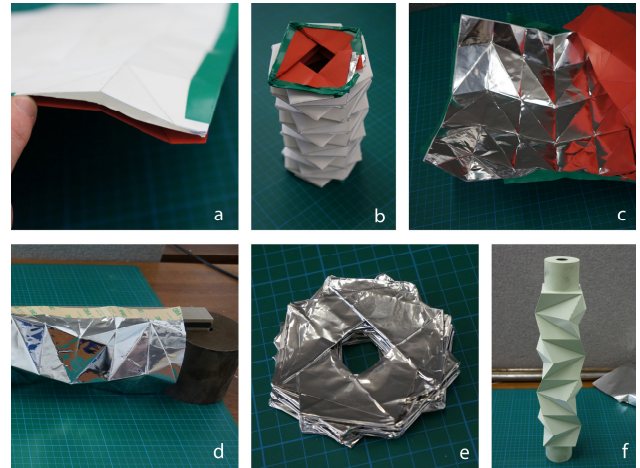


Figure 11: manufacturing process: (a) the aluminium-laminate foil is sandwiched between two pre-folded card sheets, and (b) folded into the cylindrical configuration; (c) the master sheets are removed, and the laminate sheet is (d) sealed to form a closed cylinder, before being (e) folded to its fully stowed configuration. In order to facilitate seaming of the partly-folded boom, a (f) CNC milled mandrel was manufactured.

A second manufacturing approach under consideration is to first manufacture a straight cylinder (which enables accurate alignment of the seam) followed by a controlled axial collapse of the cylinder into the desired fold pattern. Here inspiration is taken from the fact that origami folded cylinders can be considered as stable post-buckling config-

urations of axially compressed cylinders [19]. During compression, the local buckling of the boom will be controlled by means of a cylindrical master sheet that imparts the desired geometry.

An important challenge is to ensure an airtight seam for the folded cylinder. In order to facilitate the seaming, a mandrel was manufactured corresponding to partly-deployed stress-free configuration of the origami boom. Two types of seams have currently been explored: straight axial seams, and 'zig-zag' seams that follow the fold lines and thereby avoid the vertices of the fold pattern.

Deployment Experiments

An experimental set-up has been built to investigate the deployment dynamics of inflatable cylindrical booms. Inflation is done using compressed air, and a small pressure vessel provides the ability to simulate a volume-controlled deployment. Preliminary experiments have shown successful inflation and rigidisation of the origami-folded cylinders; see **Figure 12**. Initial results indicate the benefit of introducing an additional 'fake' seam to balance the section and assist straight-line deployment. However, the seams also cause local buckling after depressurization, due to the release of elastic strains. Solutions are being investigated.

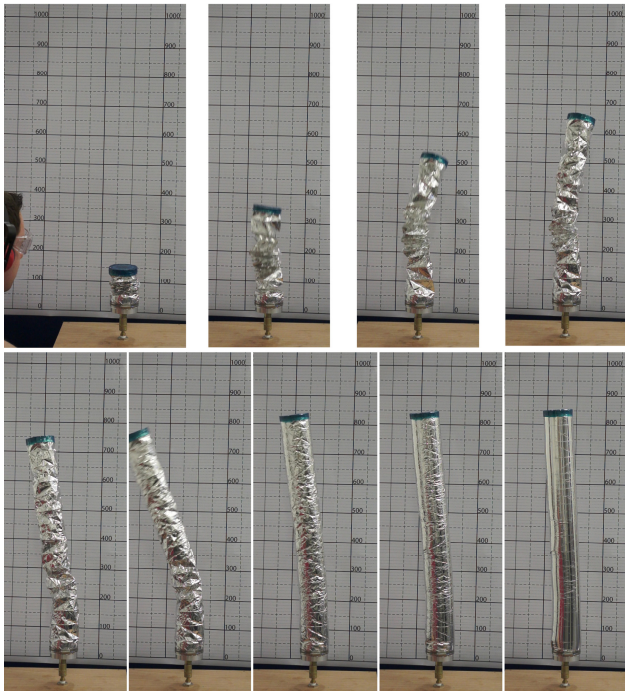


Figure 12: inflation of an origami boom (diameter 90mm) folded from aluminium-laminate foil (fold pattern $n = 4$ and $\varphi_1 = 72^\circ$).

CONCLUSION

The combination of a low weight, high packaging efficiency and a simple deployment mechanism, make inflatable structures a promising candidate for large deployable space structures. An important structural component in these structures is an inflatable cylindrical boom. One approach to compactly packaging such booms is the use of origami fold patterns: these combine compact stowage with the potential to deploy rapidly and predictably. A family of fold patterns based on a repetition of reverse folds was analysed, and a geometric incompatibility was taken as a measure of the strain during deployment. This provides a simple method to design fold patterns with less material deformation, and thereby a more predictable deployment. A series of experiments has been set up to investigate the deployment dynamics of the origami-folded inflatable booms, and establish the efficacy of strain-rigidisation of the aluminium-laminate skin in removing the creases and restoring the structural properties of the cylindrical boom.

REFERENCES

[1] Barker, R.J.P. and S.D. Guest. *Inflatable Triangulated Cylinders*. in *IUTAM-IASS Symposium on Deployable Structures: Theory and Applications*. 2000. Cambridge, UK.

[2] Fang, H. and M. Lou, *Deployment Study of a Self-Rigidizable Inflatable Boom*. *Journal of Spacecraft and Rockets*, 2006. **43**(1): p. 25-30.

[3] Freeland, R.E., et al., *Large Inflatable Deployable Antenna Flight Experiment Results*. *Acta Astronautica*, 1997. **41**: p. 267-277.

[4] Friese, G.J., G.D. Bilyeu, and M. Thomas, *Initial '80s Development of Inflated Antennas*, 1983, L'Garde Inc.

[5] Guenat, H. and O. Le Couls. *Ultra-Light Structures. Status of development & potential applications*. in *ESA Techno/Innovation Days*. 2010.

[6] Guest, S.D. and S. Pellegrino, *The Folding of Triangulated Cylinders, Part I: Geometric Considerations*. *Journal of Applied Mechanics*, 1994. **61**(4): p. 773-777.

[7] Guest, S.D. and S. Pellegrino, *The Folding of Triangulated Cylinders, Part II: The Folding Process*. *Journal of Applied Mechanics*, 1994. **61**(4): p. 778-783.

[8] Guest, S.D. and S. Pellegrino, *The Folding of Triangulated Cylinders, Part III: Experiments*. *Journal of Applied Mechanics*, 1996. **63**(1): p. 77-83.

[9] Kane, N.R., *Mathematically optimized family of ultra low distortion bellow fold patterns*, 2000, US Patent 6054194.

[10] Lacour, D., et al., *Control device for deployment of inflatable structures*, 2010, US patent 7740203.

[11] Miyazaki, Y. and M. Uchiki. *Deployment Dynamics of Inflatable Tube*. in *43rd AIAA/ASME/ASCE/AHS/ASC Structures, Structural Dynamics, and Materials Conference*. 2002. Denver, CO, USA.

[12] Nojima, T., *Modelling of Folding Patterns in Flat Membranes and Cylinders by Origami*. *JSME International Journal Series C*, 2002. **45**(1): p. 364-370.

[13] Sanders, B., et al. *Results of Qualification and Flight tests of Cool Gas Generators*. in *Space Propulsion 2010 Conference, 2-6 May 2010, San Sebastian, Spain*. 2010.

[14] Schenk, M., et al., *Review of Inflatable Booms for Deployable Space Structures: Packing and Rigidization*, 2013: submitted to the *AIAA Journal of Spacecraft and Rockets*.

[15] Senda, K., et al. *Deploy Experiment of Inflatable Tube using Work Hardening*. in *47th AIAA/ASME/ASCE/AHS/ASC Structures, Structural Dynamics, and Materials Conference*. 2006. Newport, Rhode Island, USA.

[16] Smith, S.W. and J.A. Main, *Modeling the Deployment of Inflatable Space Structures*, in *Gossamer Spacecraft: membrane and inflatable structures technology for space applications*, C.H.M. Jenkins, Editor 2000, American Institute of Aeronautics and Astronautics. p. 203-237.

[17] Sogame, A. and H. Furuya. *Conceptual Study on Cylindrical Deployable Space Structures*. in *IUTAM-IASS Symposium on Deployable Structures: Theory and Applications*. 2000. Cambridge, UK.

[18] Steele, C.R. and J.P. Fay. *Inflation of Rolled Tubes*. in *IUTAM-IASS Symposium on Deployable Structures: Theory and Applications*. 2000. Cambridge, UK.

[19] Tarnai, T. *Folding of Uniform Plane Tessellations*. in *Origami Science & Art, Proceedings of the Second International Meeting of Origami Science and Scientific Origami*. 1994. Seian University of Art and Design, Otsu, Shiga, Japan.

[20] Tsunoda, H., Y. Senbokuya, and M. Watanabe. *Deployment Method of Space Inflatable Structures Using Folding Crease Patterns*. in *44th AIAA/ASME/ASCE/AHS/ASC Structures, Structural Dynamics, and Materials Conference*. 2003. Norfolk, VA, USA.

[21] Veal, G., A. Palisoc, and W. Derbès, *Deployable inflatable boom and methods for packaging and deploying a deployable inflatable boom*, 2004.

[22] Wang, J.T. and A.R. Johnson, *Deployment Simulation Methods for Ultra-Lightweight Inflatable Structures*, 2003, NASA Langley Research Center.

[23] Wu, W., *Rigid Origami: Modelling, Application in Pre-folded Cylinders and Manufacturing*, 2010, University of Oxford.

[24] You, Z. and N. Cole. *Self-Locking Bi-Stable Deployable Booms*. in *47th AIAA/ASME/ASCE/AHS/ASC Structures, Structural Dynamics, and Materials Conference*. 2006. Newport, Rhode Island.